Theory of a two-mode micromaser simultaneously pumped by one- and two-photon atomic transitions

1999 J. Phys. B: At. Mol. Opt. Phys. 32 4405

(http://iopscience.iop.org/0953-4075/32/18/302)

J. Phys. B: At. Mol. Opt. Phys. **32** (1999) 4405–4423. Printed in the UK PII: S0953-4075(99)03397-0

Theory of a two-mode micromaser simultaneously pumped by one- and two-photon atomic transitions

David Petrosyan†‡ and P Lambropoulos†§

† Foundation for Research and Technology Hellas, Institute of Electronic Structure and Laser, PO Box 1527, Heraklion 71110, Crete, Greece
‡ Institute for Physical Research, Armenian National Academy of Sciences, Ashtarak-2, 378410, Armenia
§ Department of Physics, University of Crete, Greece
and
Max-Planck-Institut für Quantenoptik, Hans-Kopfermann-Straße 1, D-85748 Garching, Germany

Received 6 April 1999, in final form 20 July 1999

Abstract. We formulate the theory of a micromaser operating simultaneously on a one- and a two-photon atomic transition. Departing from the complete microscopic Hamiltonian for this composite 'atom plus field' system, we derive the equations governing its behaviour in the semiclassical approximation and also the fully quantum mechanical master equation. Using parameters corresponding to existing realizations of the one- and two-photon micromaser, we obtain illustrative examples of some novel aspects of this system in the steady state as well as in dynamical evolution.

1. Introduction

A rather serious experimental limitation in realizing a two-photon laser in the optical wavelength range stems from the difficulty in constructing a cavity possessing the proper finesse. The requirement is that no cavity mode is near resonance with a single-photon transition from the upper (pumped) state to an intermediate one lying between the two states connected by the desired two-photon transition. If that requirement is not satisfied, an atomic system tuned to a cavity mode on resonance with a two-photon transition will most likely lase into an adjacent mode near resonance with the single-photon transition. Thus a two-photon laser may more often than not lase simultaneously into two modes, one pumped through a single-photon transition and another pumped by the desired two-photon one. We have addressed this issue in a recent paper [1] where we have developed the theory of this unusual two-mode laser in which one of the modes is pumped by the two-photon transition.

This has motivated us to study the same problem in the context of the micromaser. Micromasers pumped by either one- or two-photon transitions have been studied quite extensively experimentally as well as theoretically [2–6]. This of course is not the place for a review of the vast literature on these topics which can be found in [7]. The difficulty with the finesse in the optical wavelength range discussed above does not arise in the two-photon micromaser because the wavelength allows the design of the appropriate cavity. For the same reason, one can envision designing a cavity which does have a second mode near resonance with the single-photon transition to an intermediate Rydberg state. It may even be possible to tune such a resonance. A further degree of flexibility in adjusting the detuning comes from

0953-4075/99/184405+19$30.00

the possibility of choosing slightly different Rydberg states. In other words, one can tune both the cavity as well as the atomic system. That is the problem we have studied in this paper; a micromaser pumped by two- and one-photon atomic transitions at the same time. Given recent progress in microcavities, one may also envision the implementation of such a system even in the context of the microlaser [8]. It is not a (micro)maser (laser) operating in two modes, but rather a (micro)maser (laser) operating in two modes one of which is inherently nonlinear.

The theory of a two- or multi-mode laser is of course a mature topic but the issue here is different in a rather fundamentally significant way. In the standard two-mode single-photon laser, the two competing modes feed on the same gain curve but each of them alone and well below threshold represents a linear process. In the present context, one of the modes exhibits a nonlinear dependence on the respective field down to zero intensity. Moreover, the two modes now feed on two different gain curves. As for the micromaser case, the issue has never been considered as it can be avoided, while for the laser, it is most often an inconvenient fact of reality. Our purpose then is to explore, in a controlled setting, the fundamental features of the resulting phenomena.

This paper is organized as follows. In section 2 we derive the effective Hamiltonian of the system, which is then used in section 3 for the analysis of the interaction of a single atom with the pure state of the cavity field. The more general master equation approach is discussed in section 4, and the formalism developed there is applied to the exploration of the semiclassical behaviour of the system in section 5, as well as its quantum-mechanical evolution in section 6. The paper is closes with the conclusions outlined in section 7.

2. Derivation of the effective Hamiltonian

The atom with the level configuration depicted in figure 1, where unperturbed atomic levels $|e\rangle$, $|i\rangle$ and $|g\rangle$ have energies $\hbar\omega_e$, $\hbar\omega_i$ and $\hbar\omega_g$, respectively, interacts with two modes of the cavity radiation field with well separated frequencies ω_a and ω_b. These frequencies are detuned from the atomic resonances by the detunings

$$\Delta_a = (\omega_i - \omega_g) - \omega_a \qquad \Delta_b = (\omega_e - \omega_i) - \omega_b \qquad (\Delta_a, \Delta_b \ll \omega_a, \omega_b) \tag{2.1}$$

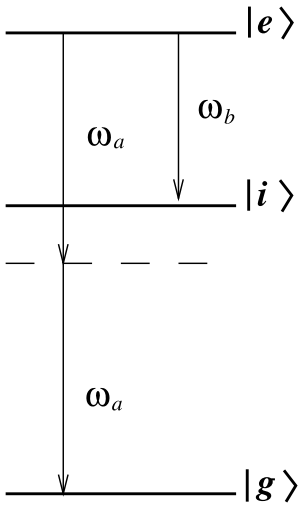

Figure 1. Schematic representation of the atomic system.

and for simplicity we assume that mode a is in perfect two-photon resonance with the atomic transition $|e\rangle \rightarrow |g\rangle$, so that $(\omega_e - \omega_i) - \omega_a = -\Delta_a$.

We begin with the complete microscopic Hamiltonian of the combined system 'atom plus cavity field', which, in the electric dipole and rotating-wave approximations, can be written as

$$H = H_{\mathrm{A}} + H_{\mathrm{F}} + H_{\mathrm{int}} \tag{2.2}$$

where H_{A}, H_{F} and H_{int} are, respectively, the atom, field and interaction terms:

$$H_{\mathrm{A}} = \hbar\omega_e|e\rangle\langle e| + \hbar\omega_i|i\rangle\langle i| + \hbar\omega_g|g\rangle\langle g| \tag{2.3}$$

$$H_{\mathrm{F}} = \hbar\omega_a\left(a^\dagger a + \tfrac{1}{2}\right) + \hbar\omega_b\left(b^\dagger b + \tfrac{1}{2}\right) \tag{2.4}$$

$$\begin{aligned} H_{\mathrm{int}} = {} & \hbar k_{ei}^{(a)}(a|e\rangle\langle i| + a^\dagger|i\rangle\langle e|) + \hbar k_{ei}^{(b)}(b|e\rangle\langle i| + b^\dagger|i\rangle\langle e|) \\ & + \hbar k_{ig}^{(a)}(a|i\rangle\langle g| + a^\dagger|g\rangle\langle i|) + \hbar k_{ig}^{(b)}(b|i\rangle\langle g| + b^\dagger|g\rangle\langle i|). \end{aligned} \tag{2.5}$$

In these equations, the field modes a and b are described, respectively, by the creation and annihilation operators $a^\dagger$, a and $b^\dagger$, b. The quantity $k_{ei}^{(a)}$ is, for instance, the coupling strength of mode a with the atomic transition $|e\rangle \rightarrow |i\rangle$, etc:

$$k_{ei}^{(a,b)} = -\frac{\langle e|D|i\rangle\mathcal{E}_{a,b}}{\hbar} \tag{2.6}$$

$$k_{ig}^{(a,b)} = -\frac{\langle i|D|g\rangle\mathcal{E}_{a,b}}{\hbar} \tag{2.7}$$

where $\langle e|D|i\rangle$ and $\langle i|D|g\rangle$ are the matrix elements of the electric dipole operator D, $\mathcal{E}_{a,b} = (\hbar\omega_{a,b}/2\epsilon_0 V)^{1/2}$ is the field per photon for the corresponding mode, and V is the cavity volume. Taking into account the fact that $\omega_a - \omega_b = \Delta_a + \Delta_b \ll \omega_{a,b}$, we can neglect the difference between $\mathcal{E}_a$ and $\mathcal{E}_b$ and drop the superscript in the coupling constants k. This simplification has practically no impact on the generality of the discussion and results which can be easily adapted to the case of two different coupling constants $k^{(a)}$, $k^{(b)}$, if that were necessary. Consistently with our model (figure 1), we assume that $|\Delta_a| \gg |\Delta_b|, k_{ei}, k_{ig}$ throughout this paper.

In the number state representation for both modes of the cavity field, the Hamiltonian (2.2) has non-vanishing matrix elements only between the following six states of the combined atom + field system: $|e, n_a, n_b\rangle$, $|i, n_a + 1, n_b\rangle$, $|i, n_a, n_b + 1\rangle$, $|g, n_a + 2, n_b\rangle$, $|g, n_a + 1, n_b + 1\rangle$ and $|g, n_a, n_b + 2\rangle$, where the first element in the kets represents the state of the atom, while the second and the third elements indicate the state of the mode a and b, respectively, containing the corresponding number of photons. We assume that a single atom initially prepared in the excited level $|e\rangle$ enters the cavity whose two modes under consideration, prior to the interaction with the atom, are in the pure number states $|n_a\rangle$ and $|n_b\rangle$, respectively. Thus, the initial state of the system is $|\psi(0)\rangle = |e, n_a, n_b\rangle$. For the moment, we assume that both cavity modes are not dumped (later on in the derivation of the master equation of the field we discuss the validity of such an assumption), which allows us to describe the system evolution using the Schrödinger equation

$$\mathrm{i}\hbar\frac{\mathrm{d}|\psi(t)\rangle}{\mathrm{d}t} = H|\psi(t)\rangle. \tag{2.8}$$

The state of the system at a subsequent time t will be represented by the linear combination of the six basis states, with the complex probability amplitudes determined by (2.8).

The differential equations for the complex probability amplitudes of the states $|i, n_a + 1, n_b\rangle$, $|g, n_a + 1, n_b + 1\rangle$ and $|g, n_a, n_b + 2\rangle$ are of the form (in the interaction picture)

$$\mathrm{i}\frac{\mathrm{d}y}{\mathrm{d}t} = \Theta y + B(t) \tag{2.9}$$

where Θ is such that $|\Theta| \gg B(t)$ (in our case Θ contains Δ_a). Equation (2.9) can be written in an integral form as

$$y(t) = -\mathrm{i}\int_0^t \mathrm{d}t' \exp[\mathrm{i}\Theta(t'-t)]B(t'). \tag{2.10}$$

For time intervals t sufficiently short, so that $B(t')$ does not change much but the exponent in (2.10) experiences many oscillations over $t' \in [0:t]$, we can integrate this equation making the slowly varying envelope approximation for $B(t)$ and, after performing the time averaging, we obtain $\langle y(t)\rangle = B(t)/\Theta$.

Following the above procedure we obtain a set of algebraic equations for the complex probability amplitudes of the states $|i, n_a+1, n_b\rangle$, $|g, n_a+1, n_b+1\rangle$ and $|g, n_a, n_b+2\rangle$. Expressing these amplitudes through the probability amplitudes A_1, A_2 and A_3 of the remaining three states $|e, n_a, n_b\rangle$, $|i, n_a, n_b+1\rangle$ and $|g, n_a+2, n_b\rangle$, respectively, we substitute them into the equations for A_1, A_2 and A_3 found from (2.8). The result is

$$\mathrm{i}\frac{\mathrm{d}A_1}{\mathrm{d}t} = -\frac{k_{ei}^2(n_a+1)}{\Delta_a}A_1 + \left(k_{ei}\sqrt{n_b+1} - \frac{k_{ei}k_{ig}^2\sqrt{(n_a+1)^2(n_b+1)}}{\Delta_a(\Delta_a+\Delta_b)}\right)A_2 - \frac{k_{ei}k_{ig}\sqrt{(n_a+1)(n_a+2)}}{\Delta_a}A_3 \tag{2.11}$$

$$\mathrm{i}\frac{\mathrm{d}A_2}{\mathrm{d}t} = \left(k_{ei}\sqrt{n_b+1} - \frac{k_{ei}k_{ig}^2\sqrt{(n_a+1)^2(n_b+1)}}{\Delta_a(\Delta_a+\Delta_b)}\right)A_1 + \left(-\Delta_b + \frac{k_{ig}^2(n_b+2)}{2(\Delta_a+\Delta_b)} + \frac{k_{ig}^2(n_a+1)}{\Delta_a+\Delta_b}\right)A_2 - \frac{k_{ig}^3\sqrt{(n_a+1)(n_a+2)(n_b+1)}}{\Delta_a(\Delta_a+\Delta_b)}A_3 \tag{2.12}$$

$$\mathrm{i}\frac{\mathrm{d}A_3}{\mathrm{d}t} = -\frac{k_{ei}k_{ig}\sqrt{(n_a+1)(n_a+2)}}{\Delta_a}A_1 - \frac{k_{ig}^3\sqrt{(n_a+1)(n_a+2)(n_b+1)}}{\Delta_a(\Delta_a+\Delta_b)}A_2 - \frac{k_{ig}^2(n_a+2)}{\Delta_a}A_3 \tag{2.13}$$

where we have dropped the term $k_{ig}^2(n_b+1)/(\Delta_a+\Delta_b)$ in the non-resonant denominators, since it is negligible in comparison with Δ_a. Now consider the physical meaning of the various terms of the above equations: first of all, we note that the terms proportional to $k^3/\Delta_a(\Delta_a+\Delta_b)$ are responsible for certain three-photon couplings between the atomic levels. Their contribution can be neglected in comparison with the first- (Ω_b) and the second- (Ω_a) order couplings

$$\Omega_a(n_a) = -\frac{k_{ei}k_{ig}\sqrt{(n_a+1)(n_a+2)}}{\Delta_a} \tag{2.14}$$

$$\Omega_b(n_b) = k_{ei}\sqrt{n_b+1} \tag{2.15}$$

since the number of photons n_a, n_b is not expected, in this context, to be so large as to violate the hierarchy of the orders of perturbation theory. This we have also checked quantitatively in detail using parameters typical for the two-photon micromaser experiments (listed later in section 5). As long as n_a and n_b are not larger than 100, these terms can be safely neglected. The terms $k_{ei}^2(n_a+1)/\Delta_a$ in (2.11), $k_{ig}^2(n_b+2)/2(\Delta_a+\Delta_b) + k_{ig}^2(n_a+1)/(\Delta_a+\Delta_b)$ in (2.12) and $k_{ei}^2(n_a+2)/\Delta_a$ in (2.13) represent the shift of the corresponding level; the n-dependent part of each term gives the Stark shift of the atomic level, whereas the remaining constant is part of the vacuum shift, which must be assumed to be incorporated into the energy of the atomic level. Under the condition $k_{ei} = k_{ig} \equiv k$, the differential Stark shift of the atomic

levels $|e\rangle$ and $|g\rangle$ vanishes and equations (2.11)–(2.13) can be greatly simplified:

$$\mathrm{i}\frac{\mathrm{d}A_1}{\mathrm{d}t} = \Omega_b(n_b)A_2 + \Omega_a(n_a)A_3 \tag{2.16}$$

$$\mathrm{i}\frac{\mathrm{d}A_2}{\mathrm{d}t} = \Omega_b(n_b)A_1 + \Delta(n_a, n_b)A_2 \tag{2.17}$$

$$\mathrm{i}\frac{\mathrm{d}A_3}{\mathrm{d}t} = \Omega_a(n_a)A_1 \tag{2.18}$$

where

$$\Delta(n_a, n_b) = -\Delta_b + \frac{k^2(4n_a + n_b)}{2(\Delta_a + \Delta_b)} \tag{2.19}$$

is the effective detuning of the mode b from the atomic transition $|e\rangle \to |i\rangle$.

Equations (2.16)–(2.18) imply the effective Hamiltonian

$$H_{\mathrm{eff}} = \hbar k(b|e\rangle\langle i| + b^{\dagger}|i\rangle\langle e|) + \hbar\mu(a^2|e\rangle\langle g| + a^{\dagger 2}|g\rangle\langle e|) \tag{2.20}$$

combined with the fact that the detuning $\Delta(n_a, n_b)$ is a function of the number of photons in both modes, a and b, of the cavity field. (In equation (2.20) the parameter $\mu = -k^2/\Delta_a$ is the coupling strength of the two-photon process.) Thus, the problem is reduced to the three-level system, and the state vector $|\psi(t)\rangle$ can be expanded at any $t \geqslant 0$ as

$$|\psi(t)\rangle = A_1(t)\,|e, n_a, n_b\rangle + A_2(t)\,|i, n_a, n_b + 1\rangle + A_3(t)\,|g, n_a + 2, n_b\rangle \tag{2.21}$$

with the initial conditions $A_1(0) = 1$, $A_2(0) = A_3(0) = 0$.

3. The energy exchange between atom and field

To find the complex probability amplitudes $A_j(t)$ ($j = 1, 2, 3$), we take the Laplace transform of the equations of motion (2.16)–(2.18). The resulting system of algebraic equations can be solved exactly, but for an arbitrary value of $\Delta(n_a, n_b)$ the procedure involves solving a cubic. In the special case of $\Delta(n_a, n_b) = 0$, this cubic factorizes and the inverse Laplace transform gives

$$A_1(t) = \cos\left(\sqrt{\Omega_a^2 + \Omega_b^2}\,t\right) \tag{3.1}$$

$$A_2(t) = -\mathrm{i}\frac{\Omega_b}{\sqrt{\Omega_a^2 + \Omega_b^2}}\sin\left(\sqrt{\Omega_a^2 + \Omega_b^2}\,t\right) \tag{3.2}$$

$$A_3(t) = -\mathrm{i}\frac{\Omega_a}{\sqrt{\Omega_a^2 + \Omega_b^2}}\sin\left(\sqrt{\Omega_a^2 + \Omega_b^2}\,t\right). \tag{3.3}$$

This shows that the population $|A_1(t)|^2$ of the atomic level $|e\rangle$ experiences Rabi oscillations with the frequency $\sqrt{\Omega_a^2 + \Omega_b^2}$. Thus, there is a periodic exchange of energy between the atom and both cavity modes. The quantity $|A_2(t)|^2$ represents the probability of adding one photon into mode b which contained n_b photons at $t = 0$. Similarly, $|A_3(t)|^2$ gives the probability for mode a to gain two photons, since each transition $|e\rangle \to |g\rangle$ leads to the emission of two photons. In figure 2 we plot the time dependence of the probabilities $|A_2(t)|^2$ and $|A_3(t)|^2$ for the case when the cavity contains initially $n_a = 10$ and $n_b = 10$ photons, using the analytical expressions (3.2) and (3.3). For comparison we plot in the same graph the probabilities $|A_2(t)|^2$ and $|A_3(t)|^2$ obtained from the numerical solution of equations (2.16)–(2.18) for the

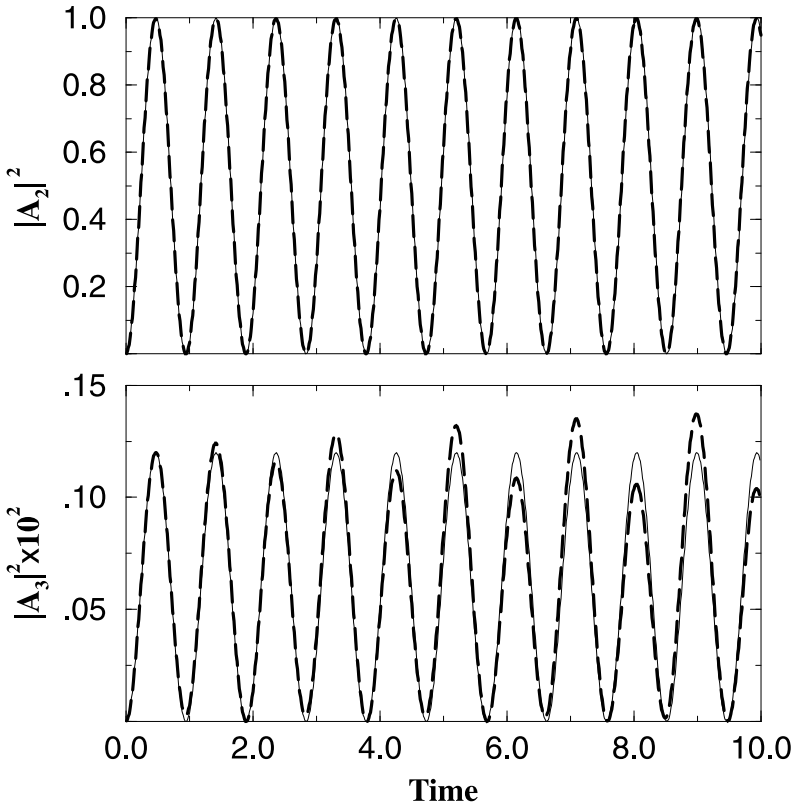

Figure 2. Time dependence of the probabilities $|A_2|^2$ and $|A_3|^2$ in the case where $n_a = n_b = 10$, obtained from the analytical expressions (3.2), (3.3) (full curves), and from the numerical solution of (2.16)–(2.18) when $\Delta_b = 0$ (broken curves). The time is measured in units of k^{-1}, $\Delta_a = 100k$.

same photon numbers and $\Delta_b = 0$. First of all, we note that the numerical solution in this case coincides almost completely with the analytical one, which is obtained under the assumption $\Delta(n_a, n_b) = 0$. This fact is easily understood from equations (2.14), (2.15) and (2.19) which show that for $\Delta_b = 0$ and not very large number of photons $n_{a,b}$, the one-photon effective detuning $\Delta(n_a, n_b)$ becomes negligible in comparison with the Rabi frequency of this transition $\Omega_b(n_b)$. Therefore, dropping the second term in (2.19) and applying for the probabilities $|A_j|^2$ equations (3.2) and (3.3) involves a very small error, and in this special case we can analyse the behaviour of the system through the analytical expressions for $|A_j|^2$.

In the absence of the detuning Δ_b, the probabilities $|A_2|^2$ and $|A_3|^2$ are proportional to the Lorentzians in front of the sines in (3.2) and (3.3), respectively, and are, therefore, determined by the Rabi frequency Ω_j of the corresponding transition. Hence, for the case of an equal number of photons in both modes, a and b, we find that the initially excited atom exchanges energy basically with the mode b only, which is coupled to the one-photon transition. The situation does not change much with the increase of the photon number in mode a, until the reasonable amount $n_a \leqslant 100$, since even in that case, the two-photon Rabi frequency still remains much smaller than the single-photon one.

To increase the two-photon transition amplitude we choose the detuning of the competing single-photon process to be appropriately large $\Delta_b = 15k$ (figure 3). In figure 3(a) we see that the amplitude of the one-photon oscillations $|A_2|^2$ is reduced significantly, whereas the

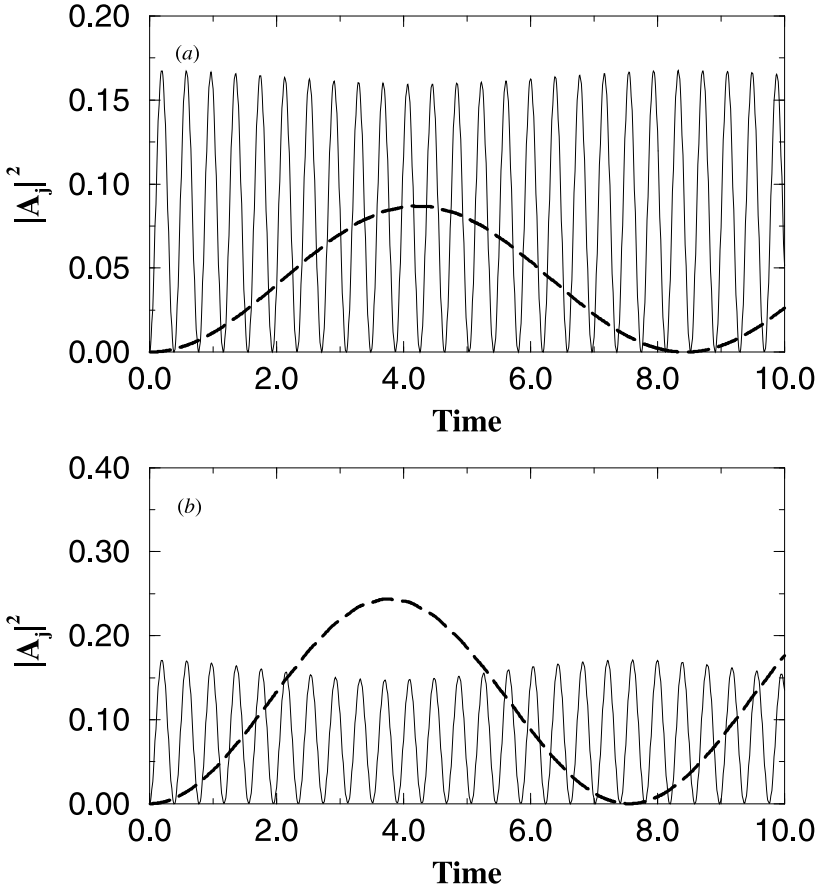

Figure 3. Time dependence of the probabilities $|A_2|^2$ (full curve) and $|A_3|^2$ (broken curve) in the case $\Delta_b = 15k$, $n_a = n_b = 10$ (*a*), and $n_a = 20$, $n_b = 10$ (*b*), obtained from the numerical solution of (2.16)–(2.18). Other parameters as in figure 2.

probability of the two-photon transition $|A_3|^2$ now oscillates with a much lower frequency but with a highly enhanced amplitude, although remaining smaller (by a factor of two) than the single-photon one. When we set $n_a = 20$ (but $n_b = 10$ still) we find that the amplitude of $|A_3(t)|^2$ is increased dramatically (figure 3(*b*)), which is due to the quadratic dependence of the two-photon transition on the field's intensity (or the photon number). On the other hand, the maximal magnitude of the one-photon oscillations amplitude is almost unchanged, although we see some amplitude modulation of the probability $|A_2|^2$ with the oscillations of $|A_3|^2$ (this effect becomes more pronounced for the larger values of $n_a > 100$). This illustrates the fact that the one-photon transition—linear in the field intensity—is rather insensitive to the existence of the competing two-photon process, except for the modulation effect, which is rather weak when $n_a, n_b < 100$. In contrast, the numerical simulations show that the two-photon transition amplitude depends strongly on the number of photons in the competing mode, which suppresses significantly the two-photon oscillations with the increase of its intensity.

Consider finally the case of a very large detuning Δ_b, so that for a given definite number of photons n_a and n_b the condition $\Omega_b(n_b) \ll \Delta(n_a, n_b)$ is satisfied. This allows us to apply

to equation (2.17) the same procedure as for equation (2.9), obtaining

$$A_2 = \frac{\Omega_b(n_b)A_1}{\Delta(n_a, n_b)} \simeq A_1 \frac{\Omega_b(n_b)}{\Delta_b} \ll 1. \tag{3.4}$$

Then the solution for the remaining two complex probability amplitudes A_1 and A_3 is found from equations (2.16) and (2.18) to be

$$A_1(t) = \cos(\Omega_a t) \tag{3.5}$$

$$A_3(t) = -\mathrm{i}\sin(\Omega_a t) \tag{3.6}$$

which describes the ordinary two-photon Rabi oscillations between the levels $|e\rangle$ and $|g\rangle$, practically unaffected by the presence of the competing mode b.

4. The master equation

In this section, we derive the general master equations for both modes of the cavity field. For this purpose, we adopt the standard micromaser assumptions [3, 4]; namely, a monoenergetic beam of excited atoms crosses the two-mode cavity at a flux low enough that, at most, one atom at a time is present inside the resonator. Let t_i be the arrival time of the ith atom and t_{int} the time spend by the atom inside the cavity. Then the assumption above implies that $t_{\mathrm{int}} \leqslant t_{i+1} - t_i$, which allows us to neglect the atom–atom interaction inside the cavity and consider the contribution of each atom independently. We also suppose that the cavity damping rate $\gamma_{a,b}$ on both frequencies ω_a and ω_b is small enough in order for the excited atoms to be able to build up the field with large number of photons: $\gamma_{a,b}^{-1} \gg t_{i+1} - t_i$. Combined with the previous inequality, this gives $t_{\mathrm{int}} \ll \gamma_{a,b}^{-1}$ and the field's relaxation process can be neglected during the time of interaction t_{int} with the single atom. With these approximations, we can adopt the standard procedure in micromaser theory [9, 10] for the derivation of the master equation of our system.

Consider first the single-atom incremental contribution to the state of the cavity field. Prior to interaction with the atom, at $t = 0$, the initial state of each mode of the cavity field can be represented quite generally as

$$\rho^{(j)}(0) = \sum_{n_j, m_j} \rho^{(j)}_{n_j, m_j}(0)|n_j\rangle\langle m_j| \qquad j = a, b. \tag{4.1}$$

The state of the atom at this moment of time is

$$\rho^{(\mathrm{at})}(0) = |e\rangle\langle e| \tag{4.2}$$

and the total density operator of the atom + field system is just a tensor product of (4.1) and (4.2):

$$\begin{aligned}\rho(0) &= \rho^{(\mathrm{at})}(0) \otimes \rho^{(a)}(0) \otimes \rho^{(b)}(0) \\ &= \sum_{n_a, m_a; n_b, m_b} \rho^{(a)}_{n_a, m_a}(0)\rho^{(b)}_{n_b, m_b}(0)|e, n_a, n_b\rangle\langle e, m_a, m_b|\end{aligned} \tag{4.3}$$

where $|e, n_a, n_b\rangle \equiv |e\rangle \otimes |n_a\rangle \otimes |n_b\rangle$.

After the interaction, at $t = t_{\mathrm{int}}$, the system evolves to the state

$$\rho(t_{\mathrm{int}}) = \sum_{n_a, m_a; n_b, m_b} \rho^{(a)}_{n_a, m_a}(0)\, \rho^{(b)}_{n_b, m_b}(0)\, |\psi_{n_a, n_b}(t_{\mathrm{int}})\rangle\langle\psi_{m_a, m_b}(t_{\mathrm{int}})| \tag{4.4}$$

where $|\psi_{n_a,n_b}(t)\rangle$ is given by equation (2.21). The state of each mode of the field at this moment of time is described by the reduced density operator

$$\rho^{(a)}(t_{\rm int}) = {\rm Tr}_b[{\rm Tr}_{at}[\rho(t_{\rm int})]] \equiv P_a(t_{\rm int})\rho^{(a)}(0) \tag{4.5}$$

$$\rho^{(b)}(t_{\rm int}) = {\rm Tr}_a[{\rm Tr}_{at}[\rho(t_{\rm int})]] \equiv P_b(t_{\rm int})\rho^{(b)}(0). \tag{4.6}$$

The pump operator $P_j(t_{\rm int})$ of mode j contains the change of the density operator $\rho^{(j)}$ of the corresponding mode due to the interaction with one single atom. Thus, if r atoms have passed through the cavity during time t, the density operator of each mode of the cavity is given by

$$\rho^{(j)}(t) = [P_j]^r \rho^{(j)}(0). \tag{4.7}$$

Equation (4.7) describes a so-called regularly pumped micromaser in the absence of decay of the cavity field. More generally, however, in the time interval between the entrance of two successive atoms in the cavity, both cavity modes decay with the corresponding rates $\gamma_{a,b}$ towards thermal equilibrium with mean numbers of thermal photons $N_{a,b}$ present in the cavity due to its coupling to the environment having a finite temperature. This process is described by the standard [9, 10] master equation

$$\begin{aligned}\frac{\rm d}{{\rm d}t}\rho^{(a)} = L\rho^{(a)} &= \tfrac{1}{2}\gamma_a(N_a+1)(2a\rho^{(a)}a^\dagger - a^\dagger a\rho^{(a)} - \rho^{(a)}a^\dagger a)\\ &+\tfrac{1}{2}\gamma_a N_a(2a^\dagger\rho^{(a)}a - aa^\dagger\rho^{(a)} - \rho^{(a)}aa^\dagger)\end{aligned} \tag{4.8}$$

and the analogous equation for $\rho^{(b)}$, with the replacement $a \leftrightarrow b$. Moreover, if the time interval $t_{i+1} - t_i$ between the two subsequent atoms fluctuates, equation (4.7) becomes inapplicable. Let the arrival times of the incoming atoms obey a Poisson distribution, which implies that the probability for an excited atom to enter the cavity between t and $t + \delta t$ is $R\,\delta t$, where $R = \langle(t_{i+1} - t_i)^{-1}\rangle$ is the average injection rate. Then, each mode of the field at time $t + \delta t$ is made up of a mixture of states corresponding to atomic excitation and no atomic excitation:

$$\rho^{(j)}(t+\delta t) = R\,\delta t\,P_j\rho^{(j)}(t) + (1 - R\,\delta t)\rho^{(j)}(t) \tag{4.9}$$

which yields, in the limit $\delta t \to 0$,

$$\frac{\rm d}{{\rm d}t}\rho^{(j)} = R[P_j\rho^{(j)}(t) - \rho^{(j)}(t)]. \tag{4.10}$$

Also including the relaxation process, we obtain, finally, the master equations governing the time evolution of both cavity modes:

$$\frac{\rm d}{{\rm d}t}\rho^{(j)} = L\rho^{(j)}(t) + R[P_j\rho^{(j)}(t) - \rho^{(j)}(t)] \qquad j = a, b \tag{4.11}$$

with $L\rho^{(j)}(t)$ given by equation (4.8). With the help of equations (4.5), (4.6) and (4.4), in the number state representation of the field, the master equations (4.11), in component form, can be written as

$$\begin{aligned}\frac{\rm d}{{\rm d}t}\rho^{(a)}_{n_a,m_a} &= -R\rho^{(a)}_{n_a,m_a}\left[1 - \sum_{n_b}\rho^{(b)}_{n_b,n_b}\sum_{z=1,2}A_z(n_a,n_b,t_{\rm int})\,A_z^*(m_a,n_b,t_{\rm int})\right]\\ &+R\rho^{(a)}_{n_a-2,m_a-2}\sum_{n_b}\rho^{(b)}_{n_b,n_b}A_3(n_a-2,n_b,t_{\rm int})\,A_3^*(m_a-2,n_b,t_{\rm int})\\ &-\tfrac{1}{2}\gamma_a[n_a+m_a+2N_a(n_a+m_a+1)]\,\rho^{(a)}_{n_a,m_a}\\ &+\gamma_a(N_a+1)\sqrt{(n_a+1)(m_a+1)}\,\rho^{(a)}_{n_a+1,m_a+1} + \gamma_a N_a\sqrt{n_a m_a}\,\rho^{(a)}_{n_a-1,m_a-1}\end{aligned} \tag{4.12}$$

for mode a, and

$$\begin{aligned}\frac{\mathrm{d}}{\mathrm{d}t}\rho^{(b)}_{n_b,m_b} = &-R\rho^{(b)}_{n_b,m_b}\left[1-\sum_{n_a}\rho^{(a)}_{n_a,n_a}\sum_{z=1,3}A_z(n_a,n_b,t_{\mathrm{int}})A^*_z(n_a,m_b,t_{\mathrm{int}})\right]\\ &+R\rho^{(b)}_{n_b-1,m_b-1}\sum_{n_a}\rho^{(a)}_{n_a,n_a}A_2(n_a,n_b-1,t_{\mathrm{int}})\,A^*_2(n_a,m_b-1,t_{\mathrm{int}})\\ &-\tfrac{1}{2}\gamma_b[n_b+m_b+2N_b(n_b+m_b+1)]\,\rho^{(b)}_{n_b,m_b}\\ &+\gamma_b(N_b+1)\sqrt{(n_b+1)(m_b+1)}\,\rho^{(b)}_{n_b+1,m_b+1}+\gamma_bN_b\sqrt{n_bm_b}\,\rho^{(b)}_{n_b-1,m_b-1}\end{aligned}\tag{4.13}$$

for mode b.

These equations imply that the interaction time t_{int} is fixed, i.e. all atoms pass through the cavity with the same speed. The generalization to the case when there is a distribution of atomic velocities is straightforward [4], but for the sake of simplicity, from now on we assume that $t_{\mathrm{int}}=$ constant.

Equations (4.12) and (4.13) are the central equations of this paper. They are similar to those one obtains for the ordinary one- and two-photon micromasers and lasers with one important new aspect: each of these equations includes the averaging over the state of the other mode.

In the following section, from equations (4.12) and (4.13) we will obtain the semiclassical evolution of the system, as well as analyse the dynamics of the photon number distribution in section 6.

5. The semiclassical evolution

Denoting by $p^{(a)}_{n_a}\equiv\rho^{(a)}_{n_a,n_a}$ and $p^{(b)}_{n_b}\equiv\rho^{(b)}_{n_b,n_b}$ the diagonal elements of the density operator of the corresponding mode of the field, from equations (4.12) and (4.13) we obtain

$$\begin{aligned}\frac{\mathrm{d}p^{(a)}_{n_a}}{\mathrm{d}t} = &-Rp^{(a)}_{n_a}\sum_{n_b}p^{(b)}_{n_b}|A_3(n_a,n_b)|^2+Rp^{(a)}_{n_a-2}\sum_{n_b}p^{(b)}_{n_b}|A_3(n_a-2,n_b)|^2\\ &-\gamma_a[n_a+N_a(2n_a+1)]p^{(a)}_{n_a}+\gamma_a(N_a+1)(n_a+1)\,p^{(a)}_{n_a+1}+\gamma_aN_an_a\,p^{(a)}_{n_a-1}\end{aligned}\tag{5.1}$$

$$\begin{aligned}\frac{\mathrm{d}p^{(b)}_{n_b}}{\mathrm{d}t} = &-Rp^{(b)}_{n_b}\sum_{n_a}p^{(a)}_{n_a}|A_2(n_a,n_b)|^2+Rp^{(b)}_{n_b-1}\sum_{n_a}p^{(a)}_{n_a}|A_2(n_a,n_b-1)|^2\\ &-\gamma_b[n_b+N_b(2n_b+1)]p^{(b)}_{n_b}+\gamma_b(N_b+1)(n_b+1)\,p^{(b)}_{n_b+1}+\gamma_bN_bn_b\,p^{(b)}_{n_b-1}\end{aligned}\tag{5.2}$$

where the explicit dependence of the probabilities $|A_j|^2$ on t_{int} has been omitted, because, as mentioned above, t_{int} is fixed.

The mean value of any physical quantity $f(n)$, which is the function of the photon number n, is given by $\langle f(n)\rangle=\sum_n p_nf(n)$. The semiclassical approximation is obtained by assuming that the photon number distribution is highly peaked around some large n, so that $\langle f(n)\rangle\simeq f(\langle n\rangle)$.

Multiplying both sides of (5.1) and (5.2) by n_a and n_b, respectively, and summing over n_a and n_b, we obtain, in the semiclassical approximation, the equations of motion for the mean photon numbers in both modes a and b:

$$\frac{\mathrm{d}\bar{n}_a}{\mathrm{d}t}=\sum_{n_a}n_a\dot{p}^{(a)}_{n_a}=2R|A_3(\bar{n}_a,\bar{n}_b)|^2-\gamma_a(\bar{n}_a-N_a)\tag{5.3}$$

$$\frac{\mathrm{d}\bar{n}_b}{\mathrm{d}t}=\sum_{n_b}n_b\dot{p}^{(b)}_{n_b}=R|A_2(\bar{n}_a,\bar{n}_b)|^2-\gamma_b(\bar{n}_b-N_b).\tag{5.4}$$

In these equations the first terms on the right-hand side represent the gain of $\bar{n}_a$ and $\bar{n}_b$ due to the downward transitions $|e\rangle \to |g\rangle$ and $|e\rangle \to |i\rangle$ of the excited atoms, respectively. The factor of 2 in (5.3) comes from the fact that each transition $|e\rangle \to |g\rangle$ causes the emission of two photons. The second terms in equations (5.3) and (5.4) are responsible for the relaxation of $\bar{n}_a$ and $\bar{n}_b$ to the mean thermal photon numbers N_a and N_b inside the cavity. If, ideally, every atom leaves the cavity in level $|i\rangle$, from equation (5.4) we find that the steady-state value for the photon number in mode b would be $\bar{n}_b = R/\gamma_b$ (providing $N_b = 0$). Similarly, from equation (5.3), in the steady state, for the maximal possible number of photons in mode a we obtain $\bar{n}_a = 2R/\gamma_a$ ($N_a = 0$).

The reader who is familiar with the theory of the homogeneously broadened two-mode laser (see, for example, [10], chapter 6) will notice a difference between the differential equations governing the intensities in that case and our equations (5.3) and (5.4). If I_1 and I_2 denote the intensities in the two modes, those equations have the form

$$\dot{I}_1 = 2I_1(a_1 - \beta_1 I_1 - \theta_{12} I_2) - \gamma_1 I_1 \tag{5.5}$$

$$\dot{I}_2 = 2I_2(a_2 - \beta_2 I_2 - \theta_{21} I_1) - \gamma_2 I_2 \tag{5.6}$$

where $a_{1,2}$ are the linear gain constants, $\beta_{1,2}$ the self-saturation coefficients, $\theta_{1,2}, \theta_{2,1}$ the cross-saturation coefficients and $\gamma_{1,2}$ the damping rate of the corresponding mode. These equations allow the two modes to oscillate independently even if $I_1 \simeq I_2$ provided $\theta_{1,2}, \theta_{2,1} < \beta_1, \beta_2$. It appears that our equations (5.3) and (5.4) do not allow for such a case (when $\Omega_a \simeq \Omega_b$) except for very short times, as can be seen by examining the form of A_2 and A_3 in equations (3.2) and (3.3) for small t, so that $\sqrt{\Omega_a^2 + \Omega_b^2}\, t \ll 1$. This seems to be a rather fundamental difference between the two systems. Of course one needs to keep in mind that atomic line broadening does not occur in the micromaser; but it is doubtful that this is the only reason for the above difference in behaviour.

Before proceeding further, let us examine the relevance of the conditions established at the beginning of section 4 to real experiments performed for the micromaser [2, 4, 6]. In a microwave cavity, with the quality factor $Q \simeq 10^8$–10^9 for both modes of the cavity field, we have for the damping rates $\gamma_{a,b} \simeq 10^2$–10^3 s^{-1}. Choosing a pump rate $R \gg \gamma_{a,b}$ ensures that many atoms pass through the cavity during its damping time; let $R = 10^5$ atom/s. In order for the atoms to be sufficiently dilute ($t_{\rm int} \leqslant R^{-1}$) we set $t_{\rm int} = 10^{-5}$ s, which is consistent with the experimental situation when atoms with thermal velocity $v \simeq 10^2$–10^3 m s^{-1} cross a cavity having a transverse dimension of about a few mm. Since the coupling constant k for Rydberg atoms is ordinarily equal to 10^5–10^6 s^{-1}, even for not very large numbers of photons $n_a, n_b \leqslant 10^2$ present in the cavity, atoms undergo many cycles of Rabi oscillations during the interaction time $t_{\rm int}$. To be definite, we choose further $\gamma_{a,b} = 10^{-2}R$, $t_{\rm int} = 10k^{-1}$ and $\Delta_a = 100k$ as before.

Consider first the case of the exact one- and two-photon resonances of modes b and a with the atomic transitions $|e\rangle \to |i\rangle$ and $|e\rangle \to |g\rangle$, respectively. It was shown in section 3, in the discussion of figure 2, that in this case during the interaction time with the cavity field, a single-atom exchanges energy primarily with mode b, so that the amplitude of the oscillations of $|A_2|^2$ is close to 1, whereas the amplitude of the oscillations of $|A_3|^2$ is a few orders of magnitude weaker, which is due to the smallness of the two-photon coupling constant μ in comparison to the one-photon matrix element k. This actually means that in equation (5.4) the gain term has a high probability to take large positive values, which depend, for fixed $t_{\rm int}$, practically only on the photon number in mode b, as is easily seen from equation (3.2) taking into account that $\Omega_a(n_a) \ll \Omega_b(n_b)$. For the same reason, with the help of equation (3.3), we deduce that, for given R, the gain term in equation (5.3) is terribly small and the only possible steady state for mode a is $\bar{n}_a = N_a$. Hence, in the case

of $\Delta_b = 0$, we recover the ordinary one-photon micromaser [3] with all its characteristic attributes.

The other limiting case, that of the pure two-photon oscillations of the system [4], can be realized in a microcavity for which the condition $\Omega_b(n_b) \ll \Delta_b$ is satisfied, as was shown at the end of section 3. This condition requires that if the detuning Δ_b is not very large, i.e. there is a mode in the microcavity close to the atomic resonance $|e\rangle \rightarrow |i\rangle$, the quality factor of the cavity on this mode should be sufficiently low. Then the maximal (possible) amount of photons in this mode $\bar{n}_b = R/\gamma_b$ would be a small number, so that the one-photon Rabi frequency $\Omega_b = k\sqrt{n_b + 1}$ is small too. Increasing the quality factor of the cavity (and consequently decreasing γ_b), to keep the above condition satisfied, one should increase the detuning Δ_b as well, making it actually very large when $\gamma_a = \gamma_b$.

It is thus interesting to consider the intermediate range of detunings Δ_b, when one would expect to observe processes caused by a real competition between modes a and b inside the cavity. For the illustration of the basic behaviour of the system in this intermediate regime,

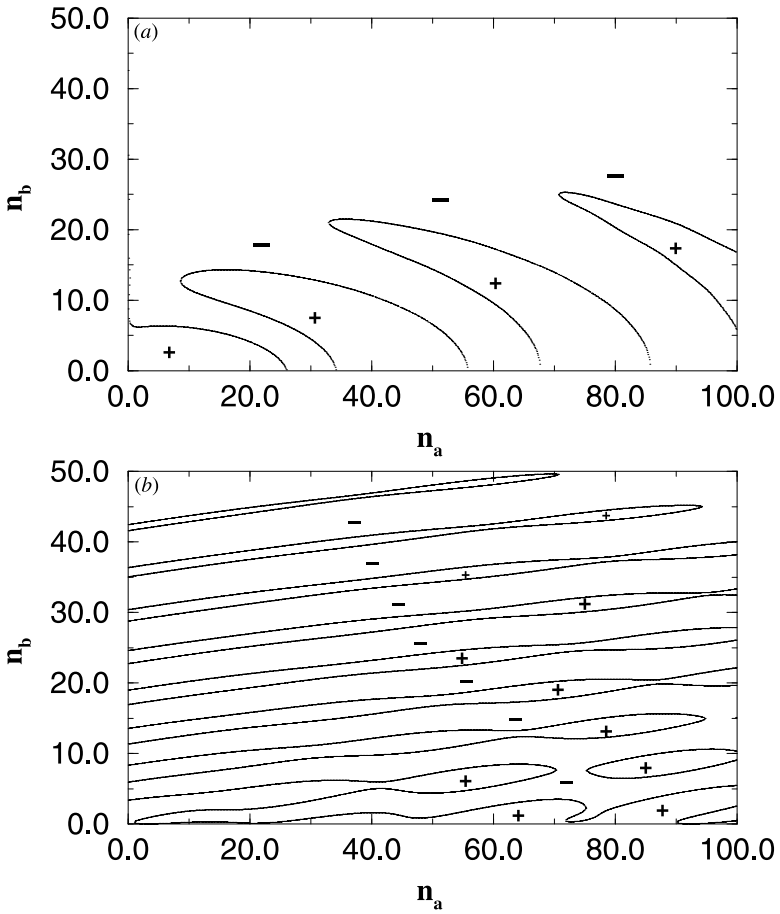

Figure 4. Diagram of the values of n_a and n_b for which $\dot{\bar{n}}_a = 0$ (*a*) and $\dot{\bar{n}}_b = 0$ (*b*). The areas marked with '+' ('−') in (*a*) and (*b*) correspond to the positive (negative) values of F_a and F_b, respectively. The mean thermal photon numbers $N_a = N_b = 0.1$, and the cavity width $\gamma_a = \gamma_b = 10^{-2}R$; other parameters are given in the text (section 5).

we choose once again $\Delta_b = 15k$ (as in section 3), since it is a rather convenient value of the single-photon process detuning.

One can formally associate the right-hand side of equations (5.3) and (5.4) with the classical force

$$F_a(n_a, n_b) \equiv 2R|A_3(n_a, n_b)|^2 - \gamma_a(n_a - N_a) \tag{5.7}$$

$$F_b(n_a, n_b) \equiv R|A_2(n_a, n_b)|^2 - \gamma_b(n_b - N_b) \tag{5.8}$$

the positive (negative) 'force' leads to the increase (decrease) of the photon number in the corresponding mode. In figure 4 we plot the diagram of the values of photon numbers in modes a and b for which $\dot{\bar{n}}_a = 0$ (figure 4(a)), and $\dot{\bar{n}}_b = 0$ (figure 4(b)), i.e. the force for the corresponding mode turns to zero. We see that there are well contoured regions of the values of n_a and n_b where the corresponding force has a definite sign. Obviously, with the decrease of the ratio of the pumping rate R to the decay rate γ_a and/or γ_b, the areas occupied by the zones of 'positive force' in the corresponding mode decrease as well, with simultaneous disappearance of the zones located around the largest values of n_a and/or n_b, respectively. The magnitude of R/γ_j for which the last positive zone in the corresponding mode j disappears (for a fixed number of photons in the other mode) can be viewed as the lasing threshold of this mode, which is, in fact, also depends on the number of photons in the competing mode.

The possible steady states of the system are given by the condition $\dot{\bar{n}}_a = \dot{\bar{n}}_b = 0$. As is seen in figure 5, this condition can be satisfied only for certain pairs n_a^s, n_b^s of the values of n_a and n_b for which the forces in both modes vanish simultaneously. To examine the stability of these steady states, we substitute $n_a = n_a^s + \delta_a$ and $n_b = n_b^s + \delta_b$, where $\delta_{a,b}$ is a small deviation from the steady state in the corresponding mode, into equations (5.3) and (5.4), respectively.

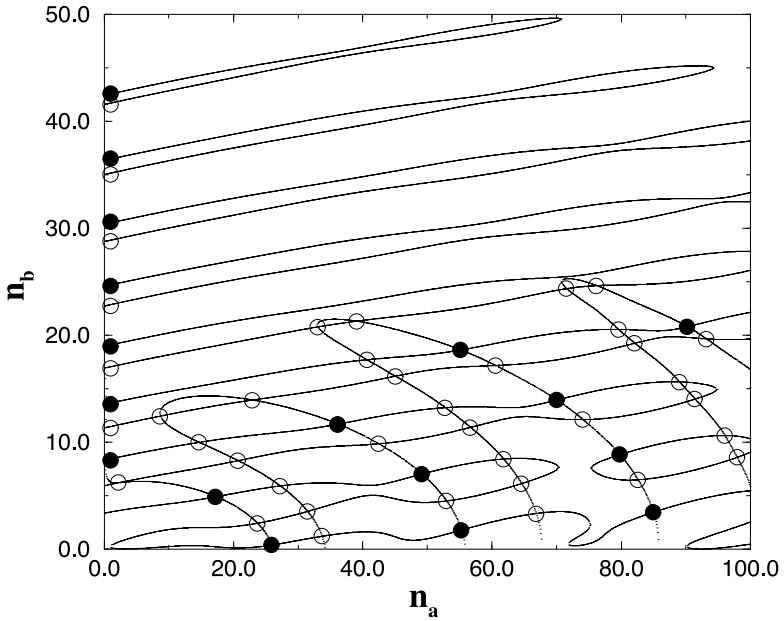

Figure 5. Diagram of the values of n_a and n_b for which the steady-state condition $\dot{\bar{n}}_a = \dot{\bar{n}}_b = 0$ is satisfied. Full circles represent the stable steady states of the system. All parameters are as in figure 4.

Applying the linearization in the parameters δ_a and δ_b, yields

$$\dot{\delta}_a = \alpha_a \delta_a + \beta_a \delta_b \tag{5.9}$$

$$\dot{\delta}_b = \alpha_b \delta_b + \beta_b \delta_a \tag{5.10}$$

where

$$\alpha_a = 2R \frac{\partial |A_3(n_a^s, n_b^s)|^2}{\partial n_a} - \gamma_a \qquad \beta_a = 2R \frac{\partial |A_3(n_a^s, n_b^s)|^2}{\partial n_b} \tag{5.11}$$

$$\alpha_b = R \frac{\partial |A_2(n_a^s, n_b^s)|^2}{\partial n_b} - \gamma_b \qquad \beta_b = R \frac{\partial |A_2(n_a^s, n_b^s)|^2}{\partial n_a}. \tag{5.12}$$

The steady-state solutions n_a^s, n_b^s are stable if, and only if, all eigenvalues of the matrix of coefficients of equations (5.9) and (5.10) have negative real parts:

$$\mathrm{Re}(\lambda_\pm) < 0 \qquad \lambda_\pm = \tfrac{1}{2}\Big[\alpha_a + \alpha_b \pm \sqrt{(\alpha_a - \alpha_b)^2 + 4\beta_a \beta_b}\,\Big]. \tag{5.13}$$

Such stable operational points of the system are plotted differently (full circles) in figure 5. Of course, if one varies the detuning Δ_b (and also, the ratio of the pumping rate R to the decays

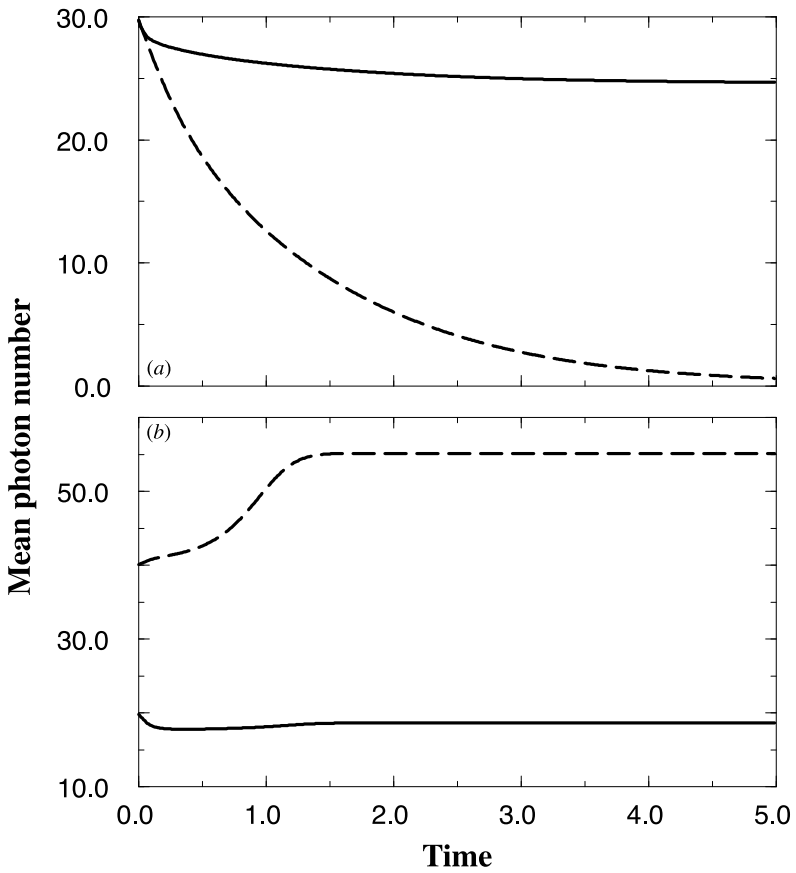

Figure 6. Time dependence of the mean photon numbers in mode a (broken curves) and b (full curves) of the cavity field. Initial conditions at time $t = 0$ are: (*a*) $\bar{n}_a = \bar{n}_b = 30$ and (*b*) $\bar{n}_a = 40$, $\bar{n}_b = 20$. The time is measured in units γ_a^{-1}. Other parameters are as in figure 4.

$\gamma_{a,b}$) one obtains different stable operational points. Within a certain range of parameters, however, the general picture of the system's behaviour remains similar, gradually tending to the appropriate limits of the limiting cases discussed above; namely, with the decrease of Δ_b the stable points tend to be located around lower values of n_a, reaching in the limit $\Delta_b \to 0$ the n_b-axis in figure 5 (one-photon maser), and vice versa for $\Delta_b \gg k$ (two-photon maser).

Finally, in figure 6, we present the semiclassical time-dependent behaviour of the system for two different 'triggering' values of the mean photon numbers in modes a and b. We see that depending on the initial conditions for $\bar{n}_a$ and $\bar{n}_b$ the system evolves towards the nearest reachable stable steady state (see figure 5). We will compare this result with the time evolution of the photon number distribution in the following section, where we present a more rigorous treatment of the system's dynamics.

6. The quantum-mechanical evolution

In this section, we present further discussion of the features of the system in terms of an exact quantum-mechanical time-dependent dynamics of the photon number distributions in modes a and b, obtained through numerical solution of equations (5.1) and (5.2).

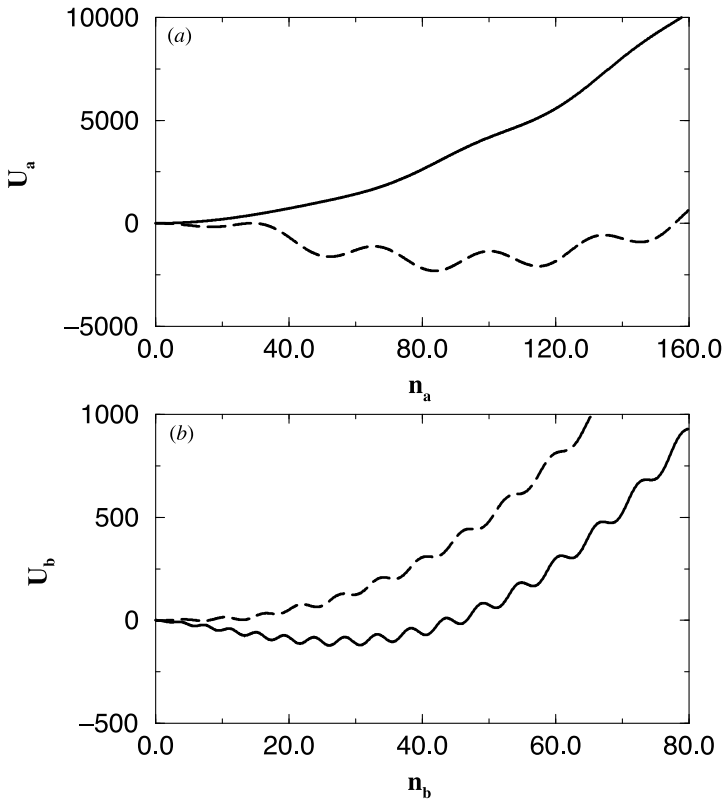

Figure 7. Potentials U_a and U_b as a function of the photon number in the corresponding mode for two different values of the detuning Δ_b: (a) potential U_a in the case $\Delta_b = 15k$, $n_b = 5$ (broken curve), and $\Delta_b = 10k$, $n_b = 30$ (full curve). (b) Potential U_b in the case $\Delta_b = 15k$, $n_a = 50$ (broken curve), and $\Delta_b = 10k$, $n_a = 5$ (full curve). Other parameters are as in figure 4.

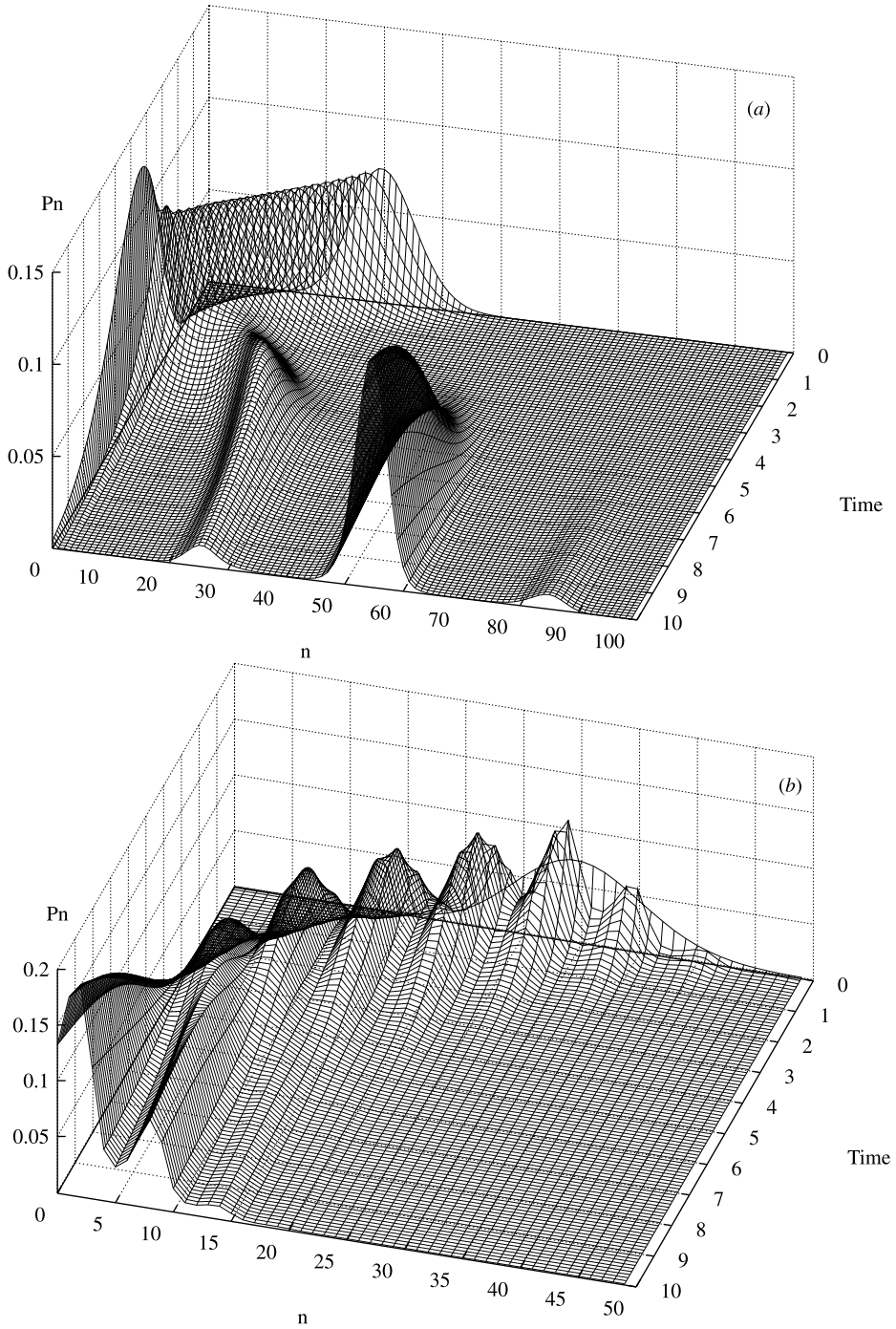

Figure 8. Time dependence of the photon number probability distribution p_n in (*a*) mode a and (*b*) mode b. Initially at time $t = 0$ both modes a and b are in coherent states centred at $n_a = n_b = 30$. All parameters are as in figure 6.

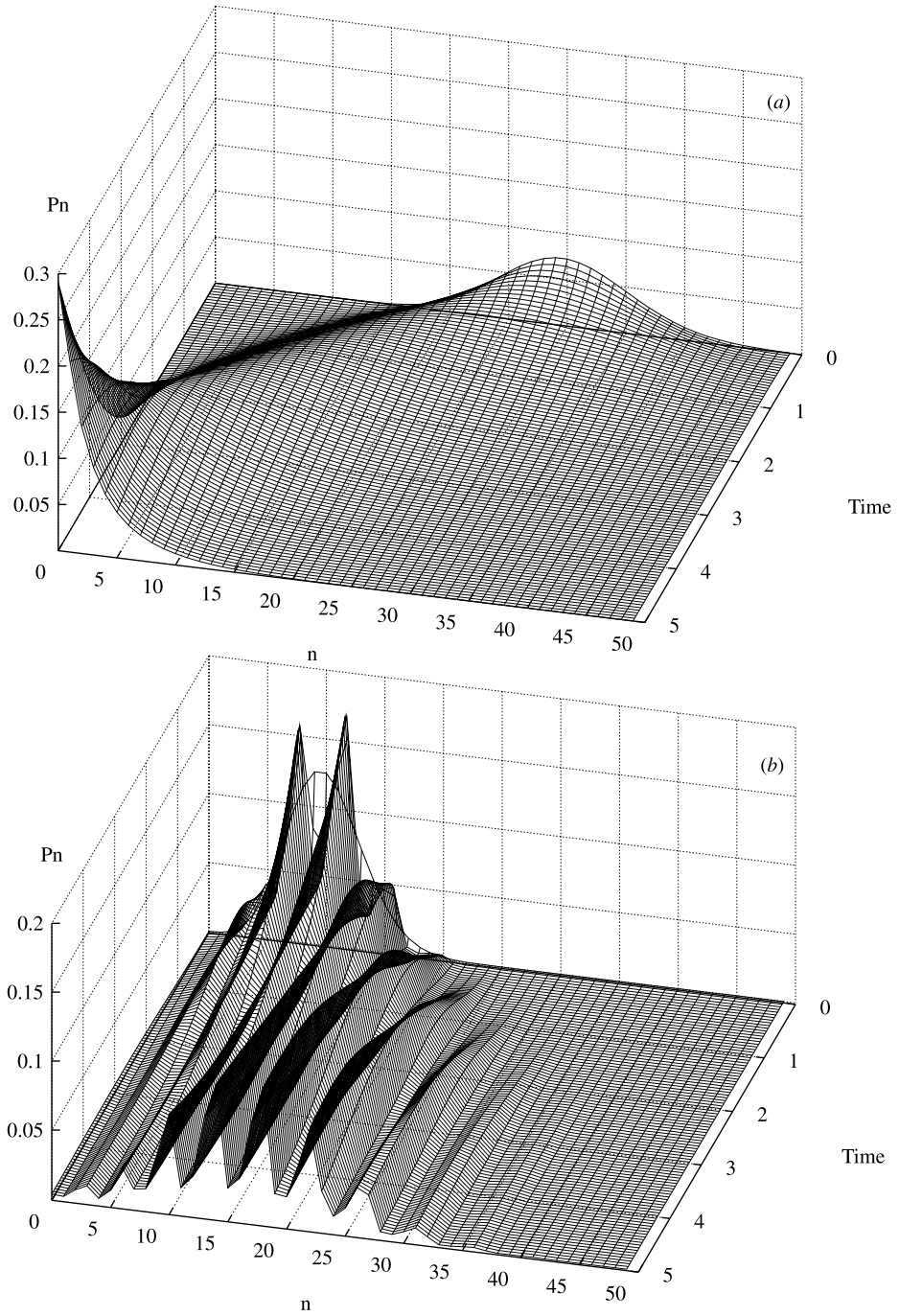

Figure 9. Time dependence of the photon number probability distribution p_n in (*a*) mode a and (*b*) mode b in the case $\Delta_b = 10$. Initially at $t = 0$ the modes a and b are in coherent states centred at $n_a = 30$ and $n_b = 10$, respectively. Other parameters are as in figure 6.

We have introduced in equations (5.7) and (5.8) the force for the corresponding mode. It is straightforward, thus, to define the potentials

$$U_a(n_a, n_b) = -\int F_a(n_a, n_b)\,\mathrm{d}n_a \tag{6.1}$$

$$U_b(n_a, n_b) = -\int F_b(n_a, n_b)\,\mathrm{d}n_b \tag{6.2}$$

which will allow us an easier interpretation of the dynamics of the system. In equation (6.1), the quantity n_b must be viewed as a parameter corresponding to the (fixed) number of photons in mode b, and similarly in equation (6.2) the parameter n_a reflects the number of photons in mode a. Numerical integration of equations (6.1) and (6.2) shows that the potential U_b of the mode b depends weakly on the parameter n_a, within the range $n_a \in [0{:}150]$ where the two-photon Rabi frequency is much weaker than the single-photon one, whereas the dependence of U_a on n_b is very strong. Physically, this means that mode b does not feel the presence of the competing two-photon transition (unless it is weak), and the behaviour of this mode is determined almost solely by its own parameters, i.e. detuning Δ_b, coupling strength k and the ratio of the pump to decay R/γ_b. The two-photon transition, in turn, apart from the system's parameters, also depends on the photon number in the one-photon mode b (see also the discussion of figure 3 in section 3). In figure 7, we plot the potentials U_a and U_b for two different values of the detuning Δ_b. Comparison with figure 6 shows that, in the semiclassical picture, the mean photon numbers $\bar{n}_a$ and $\bar{n}_b$ tend to occupy the nearest 'potential wells' of U_a and U_b, respectively. Quantum mechanically, however, although on a short time scale the evolution of the system is consistent with that given by semiclassical considerations, for longer times deviations from the latter become significant (figure 8). Apart from the local deterministic movement, the probabilities $p^{(a)}$ and $p^{(b)}$ experience a 'diffusion' through the potential barriers into the neighbouring potential minima; the lower the potential barrier, the higher the speed of this diffusion. This fact is illustrated in figures 8 and 9, which also show that the peaks of the probabilities $p^{(a)}$ and $p^{(b)}$ are located around the potential wells of U_a and U_b in figure 7. We can now specify that the time scale mentioned above refers to a diffusion time which, unlike the single-mode laser where a diffusion constant is well defined, here must be understood in reference to the results depicted in the figures. This is because an effective diffusion constant in one mode depends on the state of the other. Obviously, the diffusion intensity must be higher in the direction of the lowering of the mean potential. Thus for sufficiently long time, the photon distributions $p^{(a)}$ and $p^{(b)}$ will flow into the deepest well (global minimum) of the corresponding potential, where the steady state is reached.

7. Conclusion

In conclusion, we have explored the traditional two-photon micromaser scheme [4], in a new setting where the excited atoms pass through a cavity having two well separated modes which connect the excited atomic level to a lower level by a two-photon transition and, in addition, to an intermediate level by a single-photon one. In particular, we have explored the influence of the various parameters of the system on the probability of the amplification or suppression of the oscillations in one or the other mode of the cavity.

We have presented the derivation of the effective Hamiltonian of the system, by means of which we have illustrated the features of the interaction of the atom with the pure state of the cavity field. Further analysis of the system was carried out within the framework of the more general master equation approach through which we investigated the semiclassical behaviour of the system, as well as its quantum-mechanical evolution.

As we anticipated, this system exhibits some novel features in comparison with either the single- or the two-photon version alone. The multiple-well structure of the effective potentials associated with the forces appearing in the semiclassical analysis is one of these novel features. A number of further questions occurring in studies of the micromaser can also be explored in this new richer context with perhaps some surprises. For example, in our treatment we have seen that the effective potential for either mode is parametrically dependent on the number of photons in the other mode. It would thus be interesting to explore in this model a two-dimensional Fokker–Planck equation which would also allow for a better understanding of the diffusion of probabilities discussed in the previous section. It is also worth examining the cross-correlations between the two modes which are fed from the same upper level. Some indications of such correlations can be discerned in figure 3 and noted in the relevant discussion. We hope to report on such issues in a forthcoming paper. Finally, possible experimental studies of this system may provide valuable insight into possibilities for the optical wavelength range.

Acknowledgment

The work of one of us (DP) has been supported in part by the Republic of Armenia (scientific project no 96-770).

References

[1] Petrosyan D and Lambropoulos P 1999 *Phys. Rev.* A **60** 398
[2] Meschede D, Walther H and Müller G 1985 *Phys. Rev. Lett.* **54** 551
[3] Filipowicz P, Javanainen J and Meystre P 1986 *Phys. Rev.* A **34** 3077
[4] Brune M, Raimond J M and Haroche S 1987 *Phys. Rev.* A **35** 154
Davidovich L, Raimond J M, Brune M and Haroche S 1987 *Phys. Rev.* A **36** 3771
[5] Laughlin D W G and Swain S 1991 *Quantum Opt.* **3** 77
[6] Walther H 1996 *Usp. Fiz. Nauk.* **166** 777
[7] Haroche S and Raimond J M 1985 *Adv. At. Mol. Phys.* **20** 350
Raithel G, Wagner C, Walther H, Narducci L M and Scully M O 1994 *Cavity Quantum Electrodynamics* ed P R Bergman (Boston, MA: Academic)
[8] Feld M S and An K 1998 *Sci. Am.* **279** 41
An K, Dasari R R and Feld M S 1996 *SPIE Proc.* **2799** 14
[9] Walls D F and Milburn G J 1994 *Quantum Opt.* (Berlin: Springer)
[10] Meystre P and Sargent M III 1991 *Elements of Quantum Optics* 2nd edn (Berlin: Springer)